TOPICAL REPORT

MATHEMATICAL EXPRESSION
FOR
DROP SIZE DISTRIBUTION IN SPRAYS

by

Hiroyuki Hiroyasu

Toyota C.R.D. Lab.

Tenpaku-cho, Showa-ku

Nagoya, Japan

prepared for

NATIONAL AERONAUTICS AND SPACE ADMINISTRATION

November 1, 1967

Technical Management

NASA Lewis Research Center

Cleveland, Ohio

Chemistry and Energy Conversion Division

Paul R. Wieber

University of Wisconsin

Department of Mechanical Engineering

Madison, Wisconsin

N68 16068

MATHEMATICAL EXPRESSION

FOR

DROP SIZE DISTRIBUTION IN SPRAYS

BY

H. Hiroyasu

SUMMARY

Several mathematical expressions for the distribution of drop sizes in liquid sprays have been proposed by different researchers. These various distributions can be classified into two main types, the logarithmic normal distributions and the Chi-square distributions. In this paper, the theoretical soundness of applying these two main types of distribution functions to drop size distributions is discussed and several figures that are useful when applying them to spray data are included. It is shown how some empirical drop size distributions can be derived from the general Chi-square distribution function. This suggests that it may be possible to relate the parameters in the Chi-square distribution equation to the fundamental mechanisms of spray formation. It is concluded that the Chi-square distribution fits the available spray data well, can be graphed fairly simply, and furthermore if the parameters β and ϕ are defined, several expressions of distribution (volume, number, cumulative, etc.) can be found and several types of mean diameters can be calculated.

LIST OF SYMBOLS

A,A'	distribution constants (Table 4)
B,B'	distribution constants (Table 4)
b	distribution constant
C,C'	distribution constants (Table 4)
D,D'	distribution constants (Table 4)
$f_n(x)$	frequency distribution function of number of droplets
$f_v(x)$	frequency distribution function of volume of droplets
$I(x,\ell)$	ratio of complete and incomplete Gamma function, $\Gamma_x(\ell)/\Gamma(\ell)$
k'	distribution constant, Eq. 53
n	cumulative number fraction of droplets
N	total number of droplets in a spray
P	injection pressure
P_0	opening pressure for injection nozzle
p	droplet characteristic symbol (Table 1)
q	droplet characteristic symbol (Table 1)
r	distribution constant, Eq. 53
t	standardized normal variable (for normal distribution function)
V	total volume of droplets in a spray
v	cumulative volume of droplets
x	droplet diameter
$x^{\dagger}$	droplet size arbitrarily chosen and used to shift the coordinate scale from zero droplet size to the value x

x_{max}	maximum droplet diameter
$\bar{x}_{32}$	Sauter's mean diameter
$\bar{x}_{nm}$	number median diameter
$\bar{x}_{vm}, \bar{x}_{m}$	volume median diameter, $\bar{x}_{vm}$ used up to Eq. 13, $\bar{x}_{m}$ used thereafter, see foot note, p. 7
α	distribution constant, Eq. 51
β	chi-square distribution constant (Table 4)
$\Gamma(\ell)$	Gamma function
$\Gamma_x(\ell)$	incomplete Gamma function
δ	$1/\sqrt{2}\sigma$, Eq. 18
μ	viscosity of fuel
ρ	density of fuel
σ	standard deviation
ϕ	degree of freedom
χ^2	chi-square distribution
χ_m^2	median χ^2 value

superscripts

*	indicate normalization

subscripts

i	i-th section of droplet diameter, Eq. 14
n	number of droplets
v	volume of droplets

LIST OF FIGURES AND TABLES

MATHEMATICAL EXPRESSION
FOR
DROP SIZE DISTRIBUTION IN SPRAYS

by

H. Hiroyasu

INTRODUCTION

Various mathematical expressions for the distribution of drop sizes in liquid sprays have been proposed by different researchers. For example, the Rosin-Rammler distribution, the Nukiyama-Tanasawa distribution, the logarithmic normal distribution, the upper-limit logarithmic normal distribution and the square root normal distribution are widely used for this purpose. Unfortunately, we cannot determine which expression is theoretically best because we have no accurate method of measuring the size distribution of drops and there is little knowledge of the mechanism of droplet breakup.

Under these circumstances, a suitable expression should (1) fit the data adequately, (2) permit easy calculation of mean sizes and other mathematical parameters of interest and (3) give an insight into the fundamental mechanism of droplet production.

This paper will discuss how well the various distributions satisfy the above requirements.

THE CONCEPT OF THE DISTRIBUTIONS

There are various experimental methods of measuring the size of liquid drops sprayed from a nozzle. By these experimental methods we typically characerise a spray either by number versus diameter or by volume versus diameter (for some special cases, there is also a method for characterizing by surface area).

Let us first define the terms we shall use in describing the number and volume of drops in a spray. Speaking first of the number of droplets in a spray we define:

1.   The total number N of droplets in a spray, is mathematically defined as

$$N = \int_0^\infty f_n(x) \, dx \qquad (1)$$

where $f_n(x) = \dfrac{dn}{dx}$ and is a mathematical expression for the number of drops of a size x in a given size range dx.

2.   The cumulative number n of droplets less than a given size range x, is mathematically defined as

$$n = \int_0^x f_n(x) \, dx \qquad (2)$$

Likewise the number of droplets of a size larger than x will be given by

$$N - n = \int_x^\infty f_n(x) \, dx \qquad (3)$$

3.   The incremental number Δn of droplets in a size range between

$$x - \frac{\Delta x}{2} \quad \text{and} \quad x + \frac{\Delta x}{2} \, .$$

4.   In many cases we shall wish to normalize these terms and shall use the * superscript to indicate normalization, i.e.,

$$N^* = \int_0^\infty f_n^*(x) \, dx = 1 \qquad (4)$$

The cumulative number fraction is

$$n^* = \int_0^x f_n^*(x) \, dx \qquad (5)$$

or

$$N^* - n^* = \int_x^\infty f_n^*(x) \, dx \qquad (6)$$

We will follow the same symbolism for the volume V of N droplets in a spray using $f_v = dv/dx$ to indicate the mathematical expression for the volume of the drops in a size range dx

$$V = \int_0^\infty f_v(x)\,dx \tag{7}$$

$$v = \int_0^x f_v(x)\,dx \tag{8}$$

$$V - v = \int_x^\infty f_v(x)\,dx \tag{9}$$

The normalized expression is

$$V^* = \int_0^\infty f_v{}^*(x)\,dx = 1 \tag{10}$$

The cumulative volume fraction is

$$v^* = \int_0^x f_v{}^*(x)\,dx \tag{11}$$

or

$$V^* - v^* = \int_x^\infty f_v{}^*(x)\,dx \tag{12}$$

where the subscript v indicates a volume function as opposed to the number function f_n. Note that f_n and f_v are related by

$$f_v = \frac{\pi}{6} x^3 f_n \tag{13}$$

In some cases the cumulative volume fraction v^* is expressed as a percentage and called the percent passing volume quantity. The term percent passing volume quantity comes from the size of solid particles that would be passed through a sieve which has opening of size x. By analogy the quantity $V^* - v^*$ is sometime called the residual volume quantity.

THE CONCEPT OF MEAN DIAMETERS

In many spray problems it is desirable to work only with average diameters instead of the complete drop size distribution.

There are at least six types of mean diameters which may be used to represent a given spray distribution. This is because a spray has four characteristics, that is, the number of droplets, and the diameter, volume and surface area of each droplet.

Using these characteristics of a spray, the general equations for the various types of mean diameters can be written

$$\bar{x}_{qp} = \left(\frac{\sum x_i^q \Lambda n_i}{\sum x_i^p \Lambda n_i} \right)^{\frac{1}{q-p}} = \left(\frac{\int_0^\infty x^q f_n(x)\,dx}{\int_0^\infty x^p f_n(x)\,dx} \right)^{\frac{1}{q-p}} \tag{14}$$

where q and p may take on values corresponding to the characteristic investigated.

Some of the more important mean diameters are listed in Table 1 with the corresponding values for p and q.

TABLE 1 - MEAN AND MEDIAN DIAMETERS

	q	p			Name of Mean Diameter
$\bar{x}_{10}$	1	0	Diameter	- Number	Mean Diameter
$\bar{x}_{20}$	2	0	Surface	- Number	
$\bar{x}_{30}$	3	0	Volume	- Number	
$\bar{x}_{21}$	2	1	Surface	- Diameter	
$\bar{x}_{31}$	3	1	Volume	- Diameter	
$\bar{x}_{32}$	3	2	Volume	- Surface	Sauter's
$\bar{x}_{nm}$					Number Median Diameter
$\bar{x}_{vm}$					Volume Median Diameter

In addition to mean diameters, median diameters have also been defined. They are convenient average sizes because they can be evaluated immediately at the 50 percent mark of the cumulative distribution curves.

Two median diameters are commonly used. The first, $\bar{x}_{nm}$, is the number median diameter, i.e., the diameter of a drop such that half the total number of drops have diameters greater and half have diameters less than $\bar{x}_{nm}$, or mathematically using Eqs. 5 and 6

$$\frac{1}{2} = \int_0^{\bar{x}_{nm}} \overset{*}{f}_n(x)\,dx = \int_{\bar{x}_{nm}}^{\infty} \overset{*}{f}_n(x)\,dx = \frac{1}{2} \int_0^{\infty} \overset{*}{f}_n(x)\,dx \ . \qquad (15)$$

The second, $\bar{x}_{vm}$, is the volume (or weight) median diameter, i.e., the diameter of a drop such that half the total volume is composed of drops with diameters less than $\bar{x}_{vm}$ and half is composed of drops with diameters greater than $\bar{x}_{vm}$, defined mathematically by

$$\frac{1}{2} = \int_0^{\bar{x}_{vm}} x^3\, f_n(x)\,dx = \int_{\bar{x}_{vm}}^{\infty} x^3\, f_n(x)\,dx = \frac{1}{2} \int_0^{\infty} x^3\, f_n(x)\,dx \qquad (16)$$

LOGARITHMIC-PROBABILITY DISTRIBUTION

Most distribution functions have been defined inductively from many experimental results. To be useful, a distribution function should be well known mathematically. A normal probability distribution fits this criteria.

The normal distribution function can be adapted to give a volume distribution for sprays

$$f(x) = \frac{1}{\sqrt{2\pi}\ \sigma}\ \exp\left[\frac{-(x - x^{\dagger})^2}{2\sigma^2}\right] \qquad (17)$$

where σ is the standard deviation and $x^{\dagger}$ is called the characterizing parameter; $\overset{*}{f}_v(x)$ is maximum at $x = x^{\dagger}$.

It is found that this function gives a very poor fit to many experimental droplet distributions since they are ordinarily distributions somewhat skewed from the normal distribution. Consequently, it was suggested that the distribution be skewed from the normal function by using the logarithm of x as the variable. The first to apply the logarithmic-normal distribution to a problem of drop size distribution was Galton.[1*]

This typical logarithmic normal representation of the volume size distribution is

$$\frac{dv^*}{dy} = \frac{\delta}{\sqrt{\pi}} e^{-\delta^2 y^2} = f_v^*(x) \tag{18}$$

where

$$y = \ln\left(\frac{x}{x^\dagger}\right)$$

$$\delta = \frac{1}{\sqrt{2}\,\sigma}$$

The cumulative volume fraction is determined by integrating equation (18)

$$v^* = \frac{1}{\sqrt{\pi}} \int_{-\infty}^{z} e^{-z^2} dz \tag{19}$$

where

$$z = \delta y$$

$$v^* = \frac{1}{\sqrt{\pi}} \int_{-\infty}^{0} e^{-z^2} dz + \frac{1}{\sqrt{\pi}} \int_{0}^{z} e^{-z^2} dz \tag{20}$$

$$= \frac{1}{2} + \mathrm{erf}(z)$$

where erf(z) is the error function, or probability integral, of z.

---

*Numbers refer to references at the end of the paper.

The logarithmic normal number distribution can be shown to be

$$\frac{dn^*}{dy} = \frac{\delta}{\sqrt{\pi}} e^{-(\delta y + \frac{3}{2\delta})^2}.$$ (21)

For the $x^{\dagger}$ in the log-normal distributions, Theodore Hatch and Sarah P. Chate[2] have used the geometric mean diameter while B. Epstein[3] and F. Kottler[4] have used volume median diameter $\bar{x}_m.^{\dagger}$ Theoretically, however, we should only use the mean diameter for $x^{\dagger}$.

From equations (14) and (18) plus some algebra it can be shown that the general expression of mean diameter for this distribution is

$$\bar{x}_{qp} = x^{\dagger} \exp\left[\frac{p + q - 6}{4\delta^2}\right].$$ (22)

In the following discussion, we shall use the volume median diameter $\bar{x}_m$ for $x^{\dagger}$.

Fig. 1 shows the variation of volume distribution dv/dy with dimensionless diameter $(x/\bar{x}_m)$ for the various values of δ. From this figure, it is apparent that the logarithmic-volume distribution has a maximum point at the median diameter $\bar{x}_m$.

As it is simpler to represent volume distribution versus dimensionless diameter $(x/\bar{x}_m)$ rather than volume distribution versus the logarithm of the dimensionless diameter, we replace $dy = 1/(x/\bar{x}_m) \cdot d(x/\bar{x}_m)$ in equation (18) to obtain

$$\frac{dv^*}{d(x/\bar{x}_m)} = \frac{\delta}{\sqrt{\pi}} \frac{\bar{x}_m}{x} e^{-\delta^2(\ln(x/\bar{x}_m))^2}$$ (23)

$\dagger$ In order to write simpler expressions we hereafter write $\bar{x}_m$ to mean the same as was previously written $\bar{x}_{vm}$.

The variations of the volume distribution $dv/d(x/\bar{x}_m)$ with dimensionless diameter $(x/\bar{x}_m)$ are shown in Figure 2 for different values of δ.

Figure 3 is an example of a plot of cumulative volume on the probability scale versus $\log (x/\bar{x}_m)$. If the data follow the logarithmic-normal distribution, they will form straight lines.

The value of δ represents the degree of uniformity of the drop size in the spray, as illustrated by Figures 1, 2, and 3. The value of δ can be calculated from the slope of the lines in Figure 3, that is

$$\delta = \frac{0.394}{\log_{10}(x_{90}/\bar{x}_m)} = \frac{0.394}{\log_{10}(\bar{x}_m/x_{10})} \tag{24}$$

where x_{90} and x_{10} are the diameter for a cumulative percentage of 90 and 10 respectively.

Although the plot of an exact logarithmic-normal distribution will be a straight line on log-probability coordinates, typically the experimental data deviate from a straight line at large values of x. In an attempt to develop a different function that would not have this problem, Mugel and Evans[5] suggest an upper limit log-normal distribution which used $y = \ln(ax/(x_{max}-x))$ instead of $y = \ln(x/x^*)$ in equation (18), where x_{max} is the maximum diameter droplet in the spray.

Figure 4 illustrates the application of the upper-limit equation to Ingebo's[13] data. Here, x_{max} is determined as follows.[5] Plot the data as P against x, drawing a smooth curve to fit these points. From these curves read the 10th, 50th, and 90th percentiles, x_{10}, $x_{50} = \bar{x}_m$, and x_{90}. Then calculate x_{max} from the formula

$$x_{max} = x_{50} \cdot \frac{x_{50}(x_{90} + x_{10}) - 2 \cdot x_{90} \cdot x_{10}}{x_{50}^2 - x_{90} \cdot x_{10}} \tag{25}$$

The parameter a is readily determined from the line representing the distribution. Since y = 0 at the 50th percentile, (where $x_{50} = \bar{x}_m$, the volume median diameter), we have here

$$a = \frac{x_{max} - \bar{x}_m}{\bar{x}_m} \qquad (26)$$

The parameter δ is determined by the slope of the line, hence by any two points on it. Let us designate the coordinate on the log scale by u;

$$u = \frac{x}{x_{max} - x}$$

Then if we read the values u_{90} and u_{50} at the 90th and 50th percentiles, we find

$$\delta = \frac{0.394}{\log_{10}(u_{90}/u_{50})} \qquad (27)$$

CHI-SQUARE DISTRIBUTION

Another distribution function which can be derived from the normal distribution function is the Chi-square (χ^2) distribution. In general, if t_1, t_2, t_3, ... t_ϕ are standardized normal variables and we define

$$\chi^2 = t_1{}^2 + t_2{}^2 + t_3{}^2 + \ldots t_\phi{}^2 = \sum_{i=1}^{\phi} t_i{}^2 \qquad (28)$$

then χ^2 has the distribution

$$f(\chi^2) = \frac{1}{2^{\phi/2}\ \Gamma(\phi/2)} (\chi^2)^{\frac{\phi}{2}-1}\ e^{-\frac{\chi^2}{2}}\ d(\chi^2) \qquad (29)$$

where Γ is the Gamma function in the above equation

which is known as the χ^2 distribution with ϕ degrees of freedom.

As an illustration of the meaning of the χ^2 distribution consider a target at which we have fired a very large number of arrows. If we call the non-dimensional rectangular coordinates of a point on the target (t_1, t_2) as in Figure 5-a we can expect that the probability of a hit depends upon the radius, χ, from the target and that the frequency versus distance curves will follow a normal distribution for both t_1 and t_2 as in Fig. 5-b. Note that if the probability of a hit is the same on the t_1 and the t_2 axes, the curves in Fig. 5-b will fall on top of each other. If the probability of a hit is different between the two axes, the curves for t_1 and t_2 will not coincide as illustrated in Fig. 5-b. Now if $\chi^2 = t_1^2 + t_2^2$ as is shown in Fig. 5-a, the frequency versus χ^2 curves can be expected to follow a Chi-square distribution function with degrees of freedom $\phi = 2$ (Eq. 29) and have a shape similar to Fig. 5-c.

Another example of a form of χ^2 distribution function is the familiar Maxwell distributon of molecular velocities[6] with degrees of freedom $\phi = 3$.

The χ^2 distribution function has been applied to some problems of the distributions of droplets in sprays.[7] In this case, χ is related to the droplet diameter x by

$$\chi^2 = 2bx^{\beta},$$

where ϕ, b, and β are the distribution constants. Thus for the volume distribution the following equation is presented using Eq. 27

$$\frac{dv^*}{d\chi^2} = \frac{1}{2^{\phi/2}\Gamma(\phi/2)} (\chi^2)^{\frac{\phi}{2} - 1} e^{-\frac{\chi^2}{2}} \tag{30}$$

Since $\chi^2 = 2bx^{\beta}$, equation (30) becomes

$$\frac{dv^*}{dx} = \frac{\beta b^{\frac{\phi}{2}}}{\Gamma(\phi/2)} x^{\frac{\phi}{2}\beta - 1} e^{-bx^{\beta}} = f_v^*(x) \tag{31}$$

When $\beta = 1$, equation (31) becomes

$$\frac{dv^*}{dx} = \frac{b^{\frac{\phi}{2}}}{\Gamma(\phi/2)} \; x^{\frac{\phi}{2}-1} \; e^{-bx} . \tag{32}$$

Using $\beta = 1$ has provided a good fit to much experimental data. Equation (32) is a simple and a useful equation for drop size distributions.

The χ^2 distribution is always highly skewed for small values of ϕ, becomes more symmetric when ϕ increases, and approaches a normal distribution in shape for large ϕ as shown in Figure 6.

The number distribution corresponding to the χ^2 equation can be obtained from Eq. (31) by using the relationship between number and volume as given by Eq. (13) to give

$$\frac{dn^*}{dx} = \frac{\beta b^{(\frac{\phi}{2}-\frac{3}{\beta})}}{\Gamma(\frac{\phi}{2}-\frac{3}{\beta})} \; x^{\frac{\phi}{2}\beta - 4} \; e^{-bx^{\beta}} . \tag{33}$$

When $\beta = 1$, Eq. (33) becomes

$$\frac{dn^*}{dx} = \frac{b^{(\frac{\phi}{2}-3)}}{\Gamma(\frac{\phi}{2}-3)} \; x^{\frac{\phi}{2}-4} \; e^{-bx} \tag{34}$$

The cumulative volume fraction v^* and the cumulative number fraction n^* are determined by integrating Eqs. (30) and (33), respectively to give

$$v^* = \int_0^{\chi^2} \frac{1}{2^{\phi/2}\Gamma(\phi/2)} \; (\chi^2)^{\frac{\phi}{2}-1} \; e^{-\frac{\chi^2}{2}} \; d(\chi^2) \tag{35}$$

$$v^* = \Gamma_{2bx^{\beta}}(\phi/2) \Big/ \Gamma(\phi/2) \tag{36}$$

and

$$n^* = \Gamma_{2bx^\beta}\left(\frac{\phi}{2} - \frac{3}{\beta}\right)\bigg/ \Gamma\left(\frac{\phi}{2} - \frac{3}{\beta}\right) \tag{37}$$

where $\Gamma_x(\ell)$ is the incomplete gamma function, as defined by

$$\Gamma_x(\ell) = \int_0^x z^{\ell-1} e^{-z}\, dx \qquad \begin{array}{l} \ell > 0 \\ 0 < x < \infty \end{array}$$

Extensive tables of the ratio $I(x,\ell) = \Gamma_x(\ell)/\Gamma(\ell)$ are given in "Tables of the Incomplete Gamma Function."[8]

Then we can easily obtain the values of n^* and v^* from both the Tables of Chi-Square Distributions and from Tables of the Incomplete Gamma Function.

If we wish the commonly used Sauter's mean diameter $\bar{x}_{32}$, the value of b in Eqs. (31), (33) and related equations can be shown to be

$$b = \left[\frac{\Gamma(\phi/2)}{\Gamma\left(\frac{\phi}{2} - \frac{1}{\beta}\right)}\right]^\beta \left[\frac{1}{\bar{x}_{32}}\right]^\beta \tag{38}$$

On the other hand, if we wish the volume median diameter $\bar{x}_m$, the value of b becomes

$$b = \left[\frac{x^2_m}{2}\right]\left[\frac{1}{\bar{x}_m}\right]^\beta \tag{39}$$

where x^2_m is median χ^2 value which is discussed later.

If we introduce the dimensionless diameter as $x/\bar{x}_{32}$, then Eq. (31) may be written

$$\frac{dv^*}{d\left(\frac{x}{\bar{x}_{32}}\right)} = \beta\frac{[\Gamma(\phi/2)]^{\frac{\phi}{2}\cdot\beta-1}}{[\Gamma\left(\frac{\phi}{2} - \frac{1}{\beta}\right)]^{\beta\phi/2}}\left[\frac{x}{\bar{x}_{32}}\right]^{\frac{\phi}{2}\cdot\beta-1}\exp\left[-\frac{\Gamma(\phi/2)(x/\bar{x}_{32})}{\Gamma(\phi/2 - 1/\beta)}\right]^\beta \tag{40}$$

Since in many cases $\beta = 1$, ϕ is usually the only distribution constant. Thus, Fig. 7 shows the variation of $dv/d(\frac{x}{\bar{x}_{32}})$ with dimensionless diameter $(x/\bar{x}_{32})$ as given by Eq. 40 for various values of ϕ. The curves on this figure give a maximum point at $x/\bar{x}_{32} = 1$, that is, at Sauter's mean diameter. For this reason the form of the χ^2 distribution is very convenient.

Next, we will develop a dimensionless expression using the volume mean diameter $\bar{x}_m$. To obtain the median diameter, we define the mean value of χ^2 for each ϕ in the χ^2 distribution by the following equation

$$\int_{\chi^2_m}^{\infty} \frac{1}{2^{\phi/2}\Gamma(\phi/2)} (\chi^2)^{\frac{\phi}{2}-1} e^{-\frac{\chi^2}{2}} d(\chi^2) = \frac{1}{2} \tag{41}$$

Values of χ^2_m are listed in χ^2 distribution tables.

Thus, the relation of the median diameter to Sauter's mean diameter may be obtained from Eqs. (38) and (39)

$$\frac{\bar{x}_m}{\bar{x}_{32}} = \left[\frac{\chi^2_m}{2}\right]^{1/\beta} \frac{\Gamma(\phi/2 - 1/\beta)}{\Gamma(\phi/2)} \tag{42}$$

Table 2 shows the above relation for several values of ϕ when $\beta = 1$.

TABLE 2

ϕ	$\chi^2_m/2$	$\bar{x}_m/\bar{x}_{32}$	ϕ	$\chi^2_m/2$	$\bar{x}_m/\bar{x}_{32}$
4	1.678350	1.67835	14	6.66965	1.11161
5	2.175730	1.45092	15	7.16945	1.10299
6	2.674060	1.33703	16	7.66925	1.09561
7	3.172905	1.26917	17	8.16905	1.08921
8	3.672060	1.22402	18	8.66895	1.08362
9	4.171415	1.19183	19	9.16880	1.07868
10	4.670910	1.16773	20	9.66870	1.07430
11	5.170500	1.14900	21	10.16860	1.07039
12	5.67015	1.13403	22	10.66850	1.06685
13	6.16990	1.12180	23	11.16845	1.06366

Eq. (31) may be written with $(x/\bar{x}_m)$ by using Eq. 39 for b,

$$dv^* = \frac{\beta}{\Gamma(\phi/2)}\left[\frac{x^2_m}{2}\right]^{\phi/2}\left[\frac{x}{\bar{x}_m}\right]^{\frac{\phi}{2}\cdot\beta-1}\exp\left[-\left(\frac{x^2_m}{2}\right)\left(\frac{x}{\bar{x}_m}\right)^\beta\right]d(x/\bar{x}_m) \qquad (43)$$

If ϕ is defined, x^2_m is obtained from Table 2.

Fig. 8 shows the variation of $dv/d(x/\bar{x}_m)$ with dimensionless diameter $(x/\bar{x}_m)$ for various values of ϕ.

The value of ϕ is related to the degree of uniformity of the drop sizes in a spray, and experimental data shows ϕ is a constant for a given nozzle over a wide range of operating conditions.

When ϕ = 12, volume distribution curves for various β are shown in Fig. 9. The values of β are also associated with the degree of uniformity of drop size and it is quite sensitive to variations in drop size distribution.

Fig. 10 shows the cumulative volume distribution curves for various values of ϕ. A plot of cumulative volume distribution on a Chi-square scale against a linear $(x/\bar{x}_m)^\beta$ scale should yield a straight line for β = 1 as shown in Fig. 11.[9]

Analysis of experimental data on a liquid spray for number versus diameter distribution is easily made by converting equation (33) into the form

$$\log_{10}\left[\frac{1}{x^{\frac{\psi}{2}\cdot\beta-4}}\cdot\frac{dn}{dx}\right] = \log_{10}\left[\frac{\beta\ b^{(\frac{\phi}{2}-\frac{3}{\beta})}}{\Gamma(\frac{\phi}{2}-\frac{3}{\beta})}\right] - \frac{b}{2.3}\ x^\beta \qquad (44)$$

A plot of $\log\left[\frac{1}{x^{\frac{\psi}{2}\cdot\beta-4}}\cdot\frac{dn}{dx}\right]$ against x^β should yield a straight line with slope equal to b/2.3. Here, the values of ψ and β are determined by trial and error to give the best alignment of data points. In actual practice, construction of straight line plots from original data is quite simple, as will be illustrated later.

If we have data on the volume distribution fraction, $f_v{}^*$, we can put Eq. (31) in the form

$$\log_{10}\left[\frac{1}{x^{\frac{\phi}{2}\cdot\beta-1}}\cdot\frac{dv}{dx}\right] = \log_{10}\left[\frac{\beta\;b^{\phi/2}}{\Gamma(\phi/2)}\right] - \frac{b}{2.3}\;x^{\beta} \tag{45}$$

which expresses $\log\left[\dfrac{1}{x^{\frac{\phi}{2}\cdot\beta-1}}\cdot\dfrac{dv}{dx}\right]$ as a linear function of x^{β}.

Finally, the general equation for the mean diameter $\bar{x}_{qp}$ for the χ^2 distribution function is obtained by substituting Eq. 33 into Eq. 14 to give

$$\bar{x}_{qp}{}^{q-p} = b^{-\frac{q-p}{\beta}}\cdot\frac{\Gamma(\phi/2+(q-3)/\beta)}{\Gamma(\phi/2+(p-3)/\beta)} \tag{46}$$

When $\beta = 1$, this simplifies to

$$\bar{x}_{qp} = \frac{1}{b}\left[\frac{\Gamma(\phi/2+q-3)}{\Gamma(\phi/2+p-3)}\right]^{\frac{1}{q-p}} \tag{47}$$

If $\phi = 2$ in a χ^2 distribution equation, Eq. 31, it becomes the Rosin-Rammler equation which was presented by Rosin and Rammler[10] for application to powdered materials. That is

$$\frac{dv^*}{dx} = \beta\;bx^{\beta-1}\;e^{-bx^{\beta}} \tag{48}$$

$$v^* = \int_0^x \frac{dv^*}{dx}\;dx = e^{-bx^{\beta}} \tag{49}$$

$$V^*-v^* = 1 - e^{-bx^{\beta}} \tag{50}$$

where β and b are distribution constants. Thus the Rosin-Rammler equation can be obtained from the χ^2 distribution function.

When $\frac{\phi}{2} \cdot \beta = \alpha + 4$, the χ^2 distribution equation becomes the Nukiyama-Tanasawa equation which was empirically obtained from extensive experimental data on drop sizes in sprays formed by air atomization by S. Nukiyama and Y. Tanasawa.[11] That is, from Eqs. (31) and (33)

$$\frac{dv^*}{dx} = \frac{\beta b^{\frac{\alpha+4}{\beta}}}{\Gamma(\frac{\alpha + 4}{\beta})} x^{\alpha+3} e^{-bx^\beta} \tag{51}$$

$$\frac{dn^*}{dx} = \frac{\beta b^{\frac{\alpha+1}{\beta}}}{\Gamma(\frac{\alpha + 1}{\beta})} x^{\alpha} e^{-bx^\beta} \tag{52}$$

where α, β, and b are distribution constants. Thus, the Nukiyama-Tanasawa equation can also be obtained from the χ^2 distribution function.

Further, when $\phi/2 + 4 = r$, and $\beta = -1$, the χ^2 distribution equation Eq. (33) becomes Griffith comminution equation which was derived by L. Griffith[12] by applying the theory of probability to the molecular surface energy in an elementary comminuted system, that is

$$\frac{dn^*}{dx} = k' x^{-r} e^{-b/x} \tag{53}$$

where the values of k', r, and b can be determined from experimental data. Note that

$$k' = \frac{-b^{r-1}}{\Gamma(r-1)}$$

so that k', r, and b are related and there are really only two independent variables.

DISCUSSION AND COMPARATIVE FIT OF DISTRIBUTION EQUATIONS

The log-normal distribution and the χ^2 distribution can be compared directly in terms of their (a) mathematical characteristics (b) numerical distribution (c) volume distribution and (d) cumulative volume distribution.

Frequency, cumulative and mean diameter expressions for the log-normal distribution and chi-square distribution respectively are listed in Table 3. Dimensionless expressions of chi-square distribution are also shown in Table 4. The value of the dimensionless distribution constants for various values of ϕ and $\beta=1$ are shown in Table 5.

As discussed previously, both distributions can be obtained from normal distributions. The log-normal distribution is skewed into the normal shape by using a logarithmic abscissa, while the χ^2 distribution is formed from several normal distributions. The fact that the χ^2 distribution may be given the form of empirical drop size distribution equations suggests that it may be possible to relate the parameters in the χ^2 distribution equation to the fundamental mechanisms of spray formation.

The log-normal distribution has two parameters δ and $\bar{x}_m$, and dimensionless expressions can be made easily with $\bar{x}_m$. The χ^2 distribution has three parameters ϕ, β, and b (usually, for sprays $\beta=1$). While the χ^2 distribution can also be made nondimensional by using $\bar{x}_m$, it has the advantage of also being conveniently normalized using Sauter's mean diameter $(\bar{x}_{32})$. This is very convenient because Sauter's mean diameter has a useful physical meaning and is an important value for combustion and chemical reaction calculations. The nondimensional volume expression using $\bar{x}_{32}$ always has its maximum point at $x = \bar{x}_{32}$.

In Fig. 12, a log-normal curve (Fig. 2) is compared with a χ^2 curve (Fig. 8) of the same maximum height. Because of its broader peak, its gentler slopes near the peak, and its lower tail, the distribution frequently provides a better fit to experimental data than the log-normal distribution.

The upper-limit log-normal distribution provides a good fit to some experimental data. However, this distribution is difficult to apply because of the complications involved in determining δ and x_{max} for each set of experimental data. Because of these difficulties, the upper limit log-normal distribution is not a commonly used distribution.

TABLE 3

	Logarithmic-Normal Distribution	Chi-Square Distribution
Frequency Distribution	$$\frac{dv^*}{d(\ell n(\frac{x}{x^*}))} = \frac{\delta}{\sqrt{\pi}}\, e^{-(\delta\ \ell n(\frac{x}{x^*}))^2}$$ $$\frac{dn^*}{d(\ell n(\frac{x}{x^*}))} = \frac{\delta}{\sqrt{\pi}}\, e^{-(\delta\ \ell n(\frac{x}{x^*})+\frac{3}{2\delta})^2}$$	$$\frac{dv^*}{dx} = \frac{\beta b^{\phi/2}}{\Gamma(\phi/2)}\, x^{\frac{\phi}{2}\beta-1}\, e^{-bx^\beta}$$ $$\frac{dn^*}{dx} = \frac{\beta b^{(\frac{\phi}{2}-\frac{3}{\beta})}}{\Gamma(\frac{\phi}{2}-\frac{3}{\beta})}\, x^{\frac{\phi}{2}\beta-4}\, e^{-bx^\beta}$$
Cumulative Distribution	$$v^* = \frac{1}{\sqrt{\pi}}\int_{\infty}^{z} e^{-z^2}\, dz$$ $$z = \ell n(\frac{x}{x^*})\delta$$ (error function)	$$v^* = \int_{0}^{\chi^2} \frac{1}{2^{\frac{\phi}{2}}\,\Gamma(\frac{\phi}{2})}(\chi^2)^{\frac{\phi}{2}-1} e^{\frac{\chi^2}{2}} d(\chi^2)$$ (Chi-Square function)
Mean Diameter	$$\bar{x}_{qp} = x^*\, e^{\frac{p+q-6}{4\delta^2}}$$	$$\bar{x}_{qp}^{q-p} = b^{-\frac{q-p}{\beta}}\, \frac{\Gamma(\frac{\phi}{2}+\frac{q-3}{\beta})}{\Gamma(\frac{\phi}{2}+\frac{p-3}{\beta})}$$

TABLE 4

Dimensionless Expression of Chi-Square Distribution

$$dn^* = A\left(\frac{x}{\bar{x}_{32}}\right)^{\frac{\phi}{2}\beta-4} \exp\left(-B\left(\frac{x}{\bar{x}_{32}}\right)^{\beta}\right) d\left(\frac{x}{\bar{x}_{32}}\right)$$

$$dv^* = A'\left(\frac{x}{\bar{x}_{32}}\right)^{\frac{\phi}{2}\beta-1} \exp\left(-B'\left(\frac{x}{\bar{x}_{32}}\right)^{\beta}\right) d\left(\frac{x}{\bar{x}_{32}}\right)$$

$$dn^* = C\left(\frac{x}{\bar{x}_m}\right)^{\frac{\phi}{2}\beta-4} \exp\left(-D\left(\frac{x}{\bar{x}_m}\right)^{\beta}\right) d\left(\frac{x}{\bar{x}_m}\right)$$

$$dv^* = C'\left(\frac{x}{\bar{x}_m}\right)^{\frac{\phi}{2}\beta-1} \exp\left(-D'\left(\frac{x}{\bar{x}_m}\right)^{\beta}\right) d\left(\frac{x}{\bar{x}_m}\right)$$

where

$$A = \left[\frac{\Gamma\left(\frac{\phi}{2}\right)}{\Gamma\left(\frac{\phi}{2}-\frac{1}{\beta}\right)}\right]^{\frac{\phi}{2}\beta-3} \frac{\beta}{\Gamma\left(\frac{\phi}{2}-\frac{3}{\beta}\right)} \qquad B = \left[\frac{\Gamma\left(\frac{\phi}{2}\right)}{\Gamma\left(\frac{\phi}{2}-\frac{1}{\beta}\right)}\right]^{\beta}$$

$$A' = \beta\,\frac{\left[\Gamma\left(\frac{\phi}{2}\right)\right]^{\frac{\phi}{2}\beta-1}}{\left[\Gamma\left(\frac{\phi}{2}-\frac{1}{\beta}\right)\right]^{\frac{\phi}{2}\beta}} \qquad B' = \left[\frac{\Gamma\left(\frac{\phi}{2}\right)}{\Gamma\left(\frac{\phi}{2}-\frac{1}{\beta}\right)}\right]^{\beta}$$

$$C = \frac{\beta}{\Gamma\left(\frac{\phi}{2}-\frac{3}{\beta}\right)}\left(\frac{x_m^2}{2}\right)^{\frac{\phi}{2}-\frac{3}{\beta}} \qquad D = \frac{x_m^2}{2}$$

$$C' = \frac{\beta}{\Gamma\left(\frac{\phi}{2}\right)}\left(\frac{x_m^2}{2}\right)^{\frac{\phi}{2}} \qquad D' = \frac{x_m^2}{2}$$

TABLE 5

The Value of Dimensionless Distribution Constants shown in
Table 4 with Various ϕ ($\beta = 1$)

ϕ	A	B	A'	B'	C	D	C'	D'
7	0.8921	2.5	7.4338	2.5	1.0050	3.173	17.1208	3.173
8	3.0000	3.0	13.5000	3.0	3.6721	3.672	30.3032	3.672
9	7.3885	3.5	24.1360	3.5	9.6134	4.171	53.1658	4.171
10	16.0000	4.0	42.6667	4.0	21.8174	4.671	92.6393	4.671
11	32.3143	4.5	74.7845	4.5	45.7293	5.171	160.5360	5.171
12	62.5000	5.0	130.2086	5.0	91.1493	5.670	276.9398	5.670
13	117.4071	5.5	225.4964	5.5	175.5492	6.170	475.9812	6.170
14	216.0000	6.0	388.7988	6.0	329.8080	6.670	815.4350	6.670
15	391.2615	6.5	667.9124	6.5	608.1952	7.170	1393.1954	7.170
16	700.2918	7.0	1143.8076	7.0	1105.4847	7.670	2374.6056	7.670

The χ^2 distribution can conveniently be expressed for number frequency distribution, volume frequency distribution and cumulative distribution, but the log-normal distribution can be conveniently expressed only for cumulative volume distributions.

For example, Table 6 presents Ingebo's data[13]. He measured number versus diameter of droplet for impinging jets in a rocket combuster. The data of the third column of Table 6 n, are measured directly. From this, the data of the fourth column of Table 6, v, are calculated using the data of droplet number, i.e., third column. Fig. 13 shows these results for Run 4. From curve A it is apparent that the number frequency curve is a fairly smooth curve but the volume-frequency distribution, curve B, is irregular, i.e., the data are scattered. Because of the scattering, it is very difficult to analyze correctly for volume distribution data. Curve C of Fig. 13 is residual volume distribution data obtained from the volume fraction data. This is a fairly smooth curve, but because it was obtained from too small a sample, each data point has a large uncertainty.

The log-normal and the upper limit log-normal distributions are suited only to cumulative volume data while the χ^2 distribution can be applied directly to number frequency data as well as to cumulative volume data. For this reason the χ^2 distribution is the most generally applicable.

Figs. 14, 15, and 16 show Ingebo's data plotted for log-normal, upper limit log-normal and χ^2 distributions. Since the plot for the log-normal distribution is not a straight line, these data do not follow the log-normal distribution. While the χ^2 distribution shows some scatter, it does have the previously mentioned advantage of being able to work with volume or number distributions.

Data for one run with a small air atomizing nozzle are given by Houghton[14] as shown in Table 7. As shown in column 5, 99% of the number of droplets fall in the range of 2 $\sim$ 20 μ in diameter

TABLE 6

EXPERIMENTAL RESULTS OF INGEBO[13]

(1)   Run 4

x_μ	Δx_μ	Δn	Δv	$V^* - v^*$	$\dfrac{\Delta n}{\Delta x} \dfrac{1}{Nx^2}$	$\dfrac{x}{x_{max} - x}$
13.75	12.5	60	0.0002	1.0000	1.2675×10^{-5}	0.0617
26.25	12.5	717	0.0285	.9997	4.1537×10^{-5}	0.1223
38.75	12.5	319	0.0603	.9712	8.4830×10^{-6}	0.1957
51.25	12.5	291	0.0441	.9109	4.4227×10^{-6}	0.2763
63.75	12.5	127	0.0515	.8668	1.2475×10^{-6}	0.3686
76.25	12.5	76	0.0305	.8154	5.2196×10^{-7}	0.4752
88.75	12.5	104	0.0735	.7849	5.2710×10^{-7}	0.6000
101.25	12.5	67	0.0589	.7114	2.6090×10^{-7}	0.7475
113.75	12.5	52	0.0735	.6525	1.6043×10^{-7}	0.9251
126.25	12.5	70	0.1130	.5790	1.7532×10^{-7}	1.1429
138.75	12.5	38	0.0860	.4660	7.9835×10^{-8}	1.4164
151.25	12.5	19	0.0523	.3800	3.3154×10^{-8}	1.7698
163.75	12.5	19	0.0708	.3277	2.8278×10^{-8}	2.2444
176.25	12.5	19	0.0838	.2569	2.4417×10^{-8}	2.9152
188.75	12.5	15	0.0847	.1731	1.6806×10^{-8}	3.9356
201.25	12.5	4	0.0284	.0884	3.9426×10^{-9}	5.6754
213.75	12.5	4	0.0343	.0600	3.4950×10^{-9}	9.3097
226.25	12.5	3	0.0257	.0257	2.3433×10^{-9}	21.6300

$$x_{max} = 236.71 \; \mu \qquad dn^* = 5.3 \times 10^{-5} \; x^2 \, e^{-0.0473x} \; dx$$

$$\bar{x}_m = 137 \; \mu$$

$$x_{10} = 55 \; \mu$$

$$x_{99} = 204 \; \mu$$

TABLE 6 cont.

(2)   Run 11

x_μ	Λn	Λv	v^*-v^*	$\dfrac{\Lambda n}{\Lambda x}\dfrac{1}{Nx^2}$	$\dfrac{x}{x_{max}-x}$
13.75	1070	0.0095	1.0000	1.5518×10^{-4}	0.09776
26.25	681	.0280	.9905	2.6864×10^{-5}	0.20484
38.75	345	.0583	.9625	6.2453×10^{-6}	0.33506
51.25	343	.1068	.9042	3.5498×10^{-6}	0.49685
63.75	167	.1095	.7974	1.1169×10^{-6}	0.70325
76.25	121	.1183	.6878	5.6575×10^{-7}	0.97569
88.75	86	.1453	.5695	2.9681×10^{-7}	1.35187
101.25	68	.1575	.4242	1.8031×10^{-7}	1.90499
113.75	33	.1157	.2667	6.9327×10^{-8}	2.79828
126.25	21	.0946	.1510	3.5814×10^{-8}	4.484902
138.75	4	.0253	.0564	5.6480×10^{-9}	8.86580
151.25	4	.0311	.0311	4.7537×10^{-9}	48.0159

$$x_{max} = 154.4 \ \mu \qquad dn^* = 2.1 \times 10^{-4} \ x^2 \ e^{-0.0749x} \ dx$$

$$\bar{x}_m = 95 \ \mu$$

$$\bar{x}_{10} = 52 \ \mu$$

$$\bar{x}_{90} = 132 \ \mu$$

TABLE 6 cont.

(3)   Run 23

x_μ	Δn	Δv	$V^* - v^*$	$\frac{\Delta n}{\Delta x} \frac{1}{N x^2}$	$\frac{x}{x_{max} - x}$
13.75	78	0.0187	1.0000	1.0316×10^{-4}	0.11331
26.25	100	.0656	.9813	3.6281×10^{-5}	0.24116
38.75	61	.1360	.9157	1.0156×10^{-5}	0.40218
51.25	39	.1625	.7797	3.7122×10^{-6}	0.61121
63.75	18	.1573	.6172	1.1072×10^{-6}	0.8935
76.25	12	.1710	.4599	5.1600×10^{-7}	1.29567
88.75	8	.1628	.2889	2.5594×10^{-7}	1.91478
101.25	3	.0837	.1261	7.3156×10^{-8}	2.99113
113.75	1	.0425	.0423	1.9322×10^{-8}	5.32787

$$x_{max} = 135.1 \ \mu \qquad\qquad dn^* = 4.2 \times 10^{-4} x^2 e^{-0.0944x} dx$$

$$\bar{x}_m = 74 \ \mu$$

$$\bar{x}_{10} = 40 \ \mu$$

$$\bar{x}_{90} = 105 \ \mu$$

TABLE 7

ATOMIZATION IN A SMALL AIR-ATOMIZING NOZZLE

Data of Houghton[14]

x_μ	Δx_μ	Δn	$\Delta n/N\Delta x$	$n*$	$\Delta n/xN\Delta x$
2	2.5	390000	0.16275939	57.43	0.081379695
5	5	340000	0.07094640	82.47	0.014189280
10	5	165000	0.03442987	95.35	0.003442987
15	5	40200	0.00838837	98.31	0.000559225
20	5	11680	0.00243722	99.18	0.000121861
25	5	4970	0.00103707	99.54	0.000041483
30	5	2160	0.00045072	99.70	
35	5	1730	0.00036099	99.83	
40	5	1080	0.00022536	99.91	
45	5	650	0.00013563	99.96	
50	7.5	430	0.00005982	99.98	
60	10	350	0.00003652	99.99	
70	10	220	0.00002295	100.00	

$$dn = 0.062 \; x \; e^{-0.25x} \; dx$$

while only 1% fall in the range of $25\mu \sim 70\mu$ in diameter.

The data of 99% of droplets are plotted as shown in Fig. 17, with the result that the data are found to agree in range of $2 \sim 25\mu$ quite well with a χ^2 distribution for dn/dx when $\phi = 10$, and b = 0.25. The the distribution equation is expressed by

$$\frac{dn^*}{dx} = 0.062 \ x \ e^{-0.25x}$$

The drop size distribution produced by a particular swirl type nozzle has been measured by Edward Rice[15]. He took droplet pictures with 25 times linear magnification using a fluorescent technique. The number and size of droplets on the photographs were determined with a flying spot automatic counter.

Data for ethanol[15] is given in Table 8. The data were analyzed using the χ^2 distribution by the authors. As expected, the data follow the same dimensionless equations even if the injection pressure is changed, as shown in Fig. 18, i.e.,

$$dn^* = 0.8921 \left(\frac{x}{\bar{x}_{32}} \right)^{-0.5} e^{-2.5x} \ d\left(\frac{x}{\bar{x}_{32}} \right)$$

Thus for this nozzle the property combination the distribution is determined only by the value of Sauter's mean diameter $(\bar{x}_{32})$, and $\bar{x}_{32}$ is found to be a function of the injection pressure. This suggests that for a given nozzle and fluid property combination the distribution equation is determined by the value of $\bar{x}_{32}$ and that $\bar{x}_{32}$ might be expected, in general, to be a function of the injection pressure.

Hiroyasu and Tanasawa[16], using a new type of drop size analyzer based on sedimentation, measured the drop size distributions produced by various types of Diesel injection nozzles.

The droplets sprayed from a nozzle were allowed to fall down a settling tower onto and automatic recording balance to give weight versus time data. Then diameter versus falling time data were used with the weight versus time data to calculate the cumulative weight versus diameter distribution. Then this data was analyzed using the cumulative volume χ^2 distribution expressions.

TABLE 8

DROPLET DATA OF SWIRL ATOMIZER
OBTAINED BY EDWARD RICE[15]

P = 40 psi

x_μ	Δx_μ	Δn	$\Delta n/N\Delta x$	$x^{0.5}\Delta n/N\Delta n$
12.07	4.14	5260	9.0765×10^{-2}	3.150×10^{-1}
17.07	5.86	2278	2.7771×10^{-2}	1.147×10^{-1}
24.14	8.28	3022	2.6073×10^{-2}	1.278×10^{-1}
34.14	11.72	1270	7.7412×10^{-3}	4.521×10^{-2}
48.29	16.57	1166	5.0270×10^{-3}	3.489×10^{-2}
68.29	23.43	647	1.9727×10^{-3}	1.630×10^{-2}
96.57	33.14	222	4.7856×10^{-4}	4.695×10^{-3}
136.57	46.86	114	1.7379×10^{-4}	2.030×10^{-3}
193.14	66.27	19	2.0482×10^{-5}	2.849×10^{-4}

$$dn^* = 0.37\, x^{-0.5}\, e^{-.43x}\, dx$$

P = 70 psi

x_μ	Δx_μ	Δn	$\Delta n/N\Delta x$	$x^{0.5}\Delta n/N\Delta n$
12.07	4.14	6206	1.1976×10^{-1}	4.156×10^{-1}
17.07	5.86	2258	3.0784×10^{-2}	1.271×10^{-1}
24.14	8.28	2667	2.5733×10^{-2}	1.261×10^{-1}
34.14	11.72	730	4.9762×10^{-3}	2.906×10^{-2}
48.29	16.57	509	2.4541×10^{-3}	1.212×10^{-2}
68.29	23.43	127	4.3304×10^{-4}	3.577×10^{-3}
96.57	33.14	19	4.5804×10^{-5}	4.493×10^{-4}
136.57	46.86	1	1.7049×10^{-6}	1.991×10^{-5}

$$dn^* = 0.48\, x^{-0.5}\, e^{-0.72x}\, dx$$

TABLE 8

(continued)

P = 100 psi

x_μ	Δx_μ	Δn	$\Delta n/N\Delta x$	$x^{0.5} \, \Delta n/N\Delta x$
12.07	4.14	7752	1.386×10^{-1}	4.809×10^{-1}
17.07	5.86	2600	3.285×10^{-2}	1.357×10^{-1}
24.14	8.28	2319	2.074×10^{-2}	1.016×10^{-1}
34.14	11.72	534	3.373×10^{-3}	1.970×10^{-2}
48.29	16.57	263	1.175×10^{-3}	8.155×10^{-3}
68.29	23.43	37	1.169×10^{-4}	9.656×10^{-4}
96.57	33.14	2	4.468×10^{-6}	4.383×10^{-5}

$$dn^* = 0.59 \, x^{-0.5} \, e^{-1.09x} \, dx$$

Fig. 19 shows the effect of rotational speed of the pump on the size distribution of drops produced by a throttle nozzle. From these curves we can obtain the distribution parameters ϕ and $\bar{x}_m$. Having ϕ, the value of b can be obtained using Eq. 39 and Table 2. The results of this experiment showed that even if operating conditions are changed, the distribution parameter ϕ does not change. It was also found that the median diameter $\bar{x}_m$ of sprays decreases with increase in rotational speed, i.e., an increase of injection pressure. The expression obtained for the drop size distribution of sprays produced by a throttle nozzle is

$$dv^* = 30.30 \left(\frac{x}{\bar{x}_m}\right)^3 e^{-3.67(x/\bar{x}_m)} d(x/\bar{x}_m)$$

Similarly, the results obtained for the pintle nozzle are shown in Fig. 20, and the drop size distribution of sprays is expressed by

$$dv^* = 53.17 \left(\frac{x}{\bar{x}_m}\right)^{3.5} e^{-4.7(x/\bar{x}_m)} d(x/\bar{x}_m)$$

Fig. 22 shows the effect of viscosity of fuel on the size distribution of drops. These results show that the effect of viscosity of fuel is larger than it is usually expected to be. When the viscosity of the liquid becomes larger than 10 cp, the values of ϕ decrease with increase in viscosity as shown in Fig. 22 and ϕ takes values of $\phi = 8$ for $\mu = 10$ cp to $\phi = 4.4$ for $\mu = 200$ cp.

As has been illustrated in the above examples, experimental data show that the size distributions produced by a number of spray producing devices follow the χ^2 distribution reasonably well. This distribution can be graphed fairly simply, and furthermore, if the parameters β and ϕ are defined, several expressions of distribution (volume, number, cumulative, etc.) can be found and several mean diameters can be calculated.

ACKNOWLEDGMENT

BIBLIOGRAPHY

1) Francis Galton; Proc. Royl Soc. London, Vol 29 (1879) p. 365.

2) Theodore Hatch and Sarah P. Chate; "Statistical Description of the Size Properties of Non-Uniform Particulate Substances," J. Franklin Inst., Vol 207 (1929) pp. 369-388.

3) B. Epstein; "The Mathematical Description of Certain Breakage Mechanisms Leading to the Log-Normal Distribution," J. Franklin Inst., Vol 244 (1947) p. 471.

4) F. Kottler; "The Goodness of Fit and the Distribution of Particle Sizes," J. Franklin Inst., Vol 251 (1951) p. 499 and p. 617.

5) R.A. Mugele and H.D. Evans; "Droplet Size Distribution in Sprays," Ind. Eng. Chem., Vol 43, No. 6 (1961) pp. 1317-1324.

6) Carl A. Bennett and Normal L. Franklin; "Statistical Analysis in Chemistry and the Chemical Industry," John Wiley & Sons, Inc. (1954).

7) H. Hiroyasu, Ph.D. Thesis, Tohoku University, Japan, (1962).

8) Karl Pearson; Tables of the Incomplete Gamma Function, Cambridge University Press, (1957).

9) Y. Tanasawa; "Representation of the Size of Sprayed Drops," Kikai no Kenkyu (Japan) Vol 15, No. 12, (1963) p. 1515.

10) P. Rosin and E. Rammler; The Laws Governing the Fineness of Powdered Coal, J. of the Inst. of Fuel, Vol 7 (1933) pp. 29-36.

11) S. Nukiyama and Y. Tanasawa;"An Experiment on the Atomization of Liquid," Trans. Soc. Mech. Engrs. (Japan), Vol 4, No. 14, (1938) p. 86, Vol 4, No. 15, (1938) p. 138, Vol 5, No. 18, (1939) p. 63, Vol 6, No. 22 and No. 23 (1940).

12) L. Griffith; "A Theory of the Size Distribution of Particles in a Comminuted System" Canadian Jour. of Research, Vol 21 (1943) pp. 57-64.

13) Robert D. Ingebo and Hampton H. Foster; Drop Size Distribution for Crosscurrent Breakup, NACA TN4087 (1957).

14) H.G. Houghton; "Spray Nozzle," Chemical Engineers Handbook, J.H. Perry, New York, McGraw-Hill Co., (1965).

15) Edward J. Rice; "The Effect of Selected Fluid Parameters on Spatial Drop Size Distribution," Ph.D. Thesis, University of Wisconsin, (1966).

16) Y. Tanasawa and H. Hiroyasu, "On a Drop Size Analyzer for Liquid Sprays by Sedimentation," The Technology Reports of the Tohoku University (Japan) Vol 27, No. 1 (1962) pp. 67-89.

LOGARITHMIC-NORMAL DISTRIBUTION

$$\frac{dv^*}{dy} = \frac{\delta}{\sqrt{\pi}} e^{-\delta^2 y^2}$$

$$y = \ln\left(\frac{x}{x_m}\right)$$

$\delta = 0.5$

$\delta = 1.0$

$\delta = 1.6$

$\delta = 2.0$

$\delta = 3.0$

dv^*/dy

x/x_m

Fig. 1

LOGARITHMIC-NORMAL DISTRIBUTION

$$\frac{dv^*}{d(\frac{x}{\bar{x}_m})} = \frac{\delta}{\sqrt{\pi}}(\frac{\bar{x}_m}{x})e^{-\delta^2 (\ln(\frac{x}{\bar{x}_m}))^2}$$

$\delta = 3.0$

$\delta = 2.0$

$\delta = 1.6$

$\delta = 1.0$

$\delta = 0.5$

$dv^*/d(\frac{x}{\bar{x}_m})$

x/$\bar{x}_m$

Fig. 2

Fig. 3

Fig. 4

The figure shows a plot of CUMULATIVE VOLUME v* (vertical axis, ranging from .0001 to .9999) versus $u = \dfrac{x}{x_{max} - x}$ (horizontal axis, ranging from 0.1 to 10.0).

INGEBO'S DATA
RUN 4

$X_{10} = 55.0\mu$
$X_{90} = 204.0\mu$
$\bar{X}_{50} = 135.0\mu$
$X_{max} = 236.71\mu$
$\delta = 0.63$

Fig. 5a

NUMBER

DISTANCE FROM CENTER (t_1, t_2)

Fig. 5b

t_2

t_1

NUMBER

χ^2-DISTRIBUTION
($\phi = 2$)

DISTANCE (χ)

Fig. 5c

$$\frac{dv^*}{d(\chi^2)} = \frac{1}{2^{\frac{\phi}{2}}\Gamma\frac{\phi}{2}}(\chi^2)^{\frac{\phi}{2}-1} e^{-\frac{\chi^2}{2}}$$

$\phi=2$

$\phi=4$

$\phi=6$

$\phi=8$

$\phi=10$

$\phi=14$

$\phi=20$

$\phi=30$

$dv^*/d\chi^2$

χ^2

Fig. 6

$$dv^* = A\left(\frac{x}{\bar{x}_{32}}\right)^{\frac{\phi}{2}\beta-1} e^{-B\left(\frac{x}{\bar{x}_{32}}\right)^{\beta}} d\left(\frac{x}{\bar{x}_{32}}\right), \quad \beta=1$$

$$A = \left[\frac{\Gamma\left(\frac{\phi}{2}\right)}{\Gamma\left(\frac{\phi}{2}-1\right)}\right]^{\frac{\phi}{2}-3} \cdot \frac{1}{\Gamma\left(\frac{\phi}{2}-3\right)}$$

$$B = \left[\frac{\Gamma\left(\frac{\phi}{2}\right)}{\Gamma\left(\frac{\phi}{2}-1\right)}\right]$$

$\phi=18$
16
14
12
10
8

$\phi=4$
$\phi=6$

Vertical axis: $dv^*/d(x/\bar{x}_{32})$ with values 0, 0.2, 0.4, 0.6, 0.8, 1.0, 1.2

Horizontal axis: $x/\bar{x}_{32}$ with values 0, 1.0, 2.0, 3.0, 4.0

Fig. 7

$$dv^* = A'\left(\frac{x}{\bar{x}_m}\right)^{\frac{\phi}{2}\cdot\beta-1} e^{-B'\left(\frac{x}{\bar{x}_m}\right)^{\beta}} d\left(\frac{x}{\bar{x}_m}\right)$$

$$A' = \frac{\left[\Gamma\left(\frac{\phi}{2}\right)\right]^{\frac{\phi}{2}-1}}{\left[\Gamma\left(\frac{\phi}{2}-1\right)\right]^{\frac{\phi}{2}}}, \quad B' = \left[\frac{\Gamma\left(\frac{\phi}{2}\right)}{\Gamma\left(\frac{\phi}{2}-1\right)}\right], \quad \beta = 1$$

$\phi = 18$
16
14
12
10
8
6
$\phi = 4$

$dv^*/d(x/\bar{x}_m)$

$x/\bar{x}_m$

Fig. 8

$$dv^* = A' \left(\frac{x}{\bar{x}_m} \right)^{\frac{\phi}{2} \cdot \beta - 1} e^{-\left[B' \left(\frac{x}{\bar{x}_m} \right)^\beta \right]} d\left(\frac{x}{\bar{x}_m} \right)$$

$$\phi = 12, \quad A' = \beta \frac{120\beta - 1}{\left[\Gamma\left(6 - \frac{1}{\beta} \right) \right]^{6\beta}}$$

$$B' = \left[\frac{120}{\Gamma\left(6 - \frac{1}{\beta} \right)} \right]^\beta$$

$\beta = 2$

$\beta = 1$

$\beta = \frac{1}{3}$

$\beta = \frac{1}{2}$

$\dfrac{x}{\bar{x}_m}$

Fig. 9

CUMULATIVE VOLUME v*

CHI-SQUARE DISTRIBUTION

$x/\bar{x}_m$

Fig. 10

Fig. II

$dv*/d\left(\dfrac{x}{\bar{x}_m}\right)$

1.2
1.0
0.8
0.6
0.4
0.2
0

CHI-SQUARE DISTRIBUTION
$\phi = 12, \beta = 1$ (Eq. 43)

LOG-NORMAL DISTRIBUTION
$\delta = 1.6$ (Eq. 23)

0
1.0
2.0
3.0

DROP DIAMETER $x/\bar{x}_m$

Fig. 12

INGEBO'S DATA

□ CUMULATIVE VOLUME vs DIAMETER
○ NUMBER vs DIAMETER
△ VOLUME vs DIAMETER

DROP DIAMETER x μ

Fig. 13

INGEBO'S DATA
o RUN 4
△ RUN II
□ RUN 23

RUN 23

RUN II

RUN 4

CUMULATIVE VOLUME v*

DROP DIAMETER x_μ

Fig. 14

Fig. 15

INGEBO'S DATA

Run	Air Vel.	
o 4	100 ft/sec	$dn = 5.3 \times 10^{-5} x^2 e^{-0.0473x} dx$
△ 11	180	$dn = 2.1 \times 10^{-4} x^2 e^{-0.0749x} dx$
□ 23	300	$dn = 4.2 \times 10^{-4} x^2 e^{-0.0944x} dx$

RUN 4

RUN 11

RUN 23

$\dfrac{1}{x^2} \cdot \dfrac{\Delta n}{n} \cdot \dfrac{1}{\Delta x}$

DROP DIAMETER $x\mu$

Fig. 16

HOUGHTON'S DATA

$$\frac{dn^*}{dx} = 0.062 \times e^{-0.25x}$$

Fig. 17

RICE'S DATA
○ P = 40 psi $\bar{x}_{32} = 58.1\mu$
△ P = 70 psi $\bar{x}_{32} = 34.5\mu$
□ P = 100 psi $\bar{x}_{32} = 22.9\mu$

$$dn^* = 0.892\left(\frac{x}{\bar{x}_{32}}\right)^{-0.5} e^{-2.5x}\, d\left(\frac{x}{\bar{x}_{32}}\right)$$

P = 40 psi

P = 70 psi

P = 100 psi

$\frac{\Delta n}{N\Delta x} \cdot x 0.5$

DROP DIAMETER $x\mu$

Fig. 18

Fig. 19

The figure is rotated 90°. The plot shows CUMULATIVE VOLUME $V^* - v^*$ on the vertical axis (1.00, .75, .50, .25) versus DROPLET DIAMETER x_μ on the horizontal axis (0 to 200).

Legend / annotations:
$\phi = 8, \beta = 1$

THROTTLE NOZZLE ($P_0 = 100 kg/cm^2$)
$\mu = 10$ cP
$r = 21$ mm

o $n = 300$ rpm
△ $n = 500$
□ $n = 750$
◊ $n = 1000$

$\bar{x}_m = 59.2$
$\bar{x}_m = 55.6$
$\bar{x}_m = 53.2$
$\bar{x}_m = 51.7$

Fig. 20

PINTLE NOZZLE (P_0=100kg/cm²)

ϕ=7, β=1

μ=10 cP
r=21mm

o	n=300 rpm	
△	n=500	
□	n=750	
φ	n=1000	

$\bar{x}_m$=64.8
$\bar{x}_m$=62.2
$\bar{x}_m$=58.8
$\bar{x}_m$=55.7

CUMULATIVE VOLUME V^*-v^*

DROPLET DIAMETER x_μ

Fig. 21

CUMULATIVE VOLUME V*-v*

THROTTLE NOZZLE (P₀=100kg/cm²)

n = 500 rpm
r = 21mm

○ μ=225.4 cP
△ μ=114.7
□ μ=50.0
▽ μ=22.5
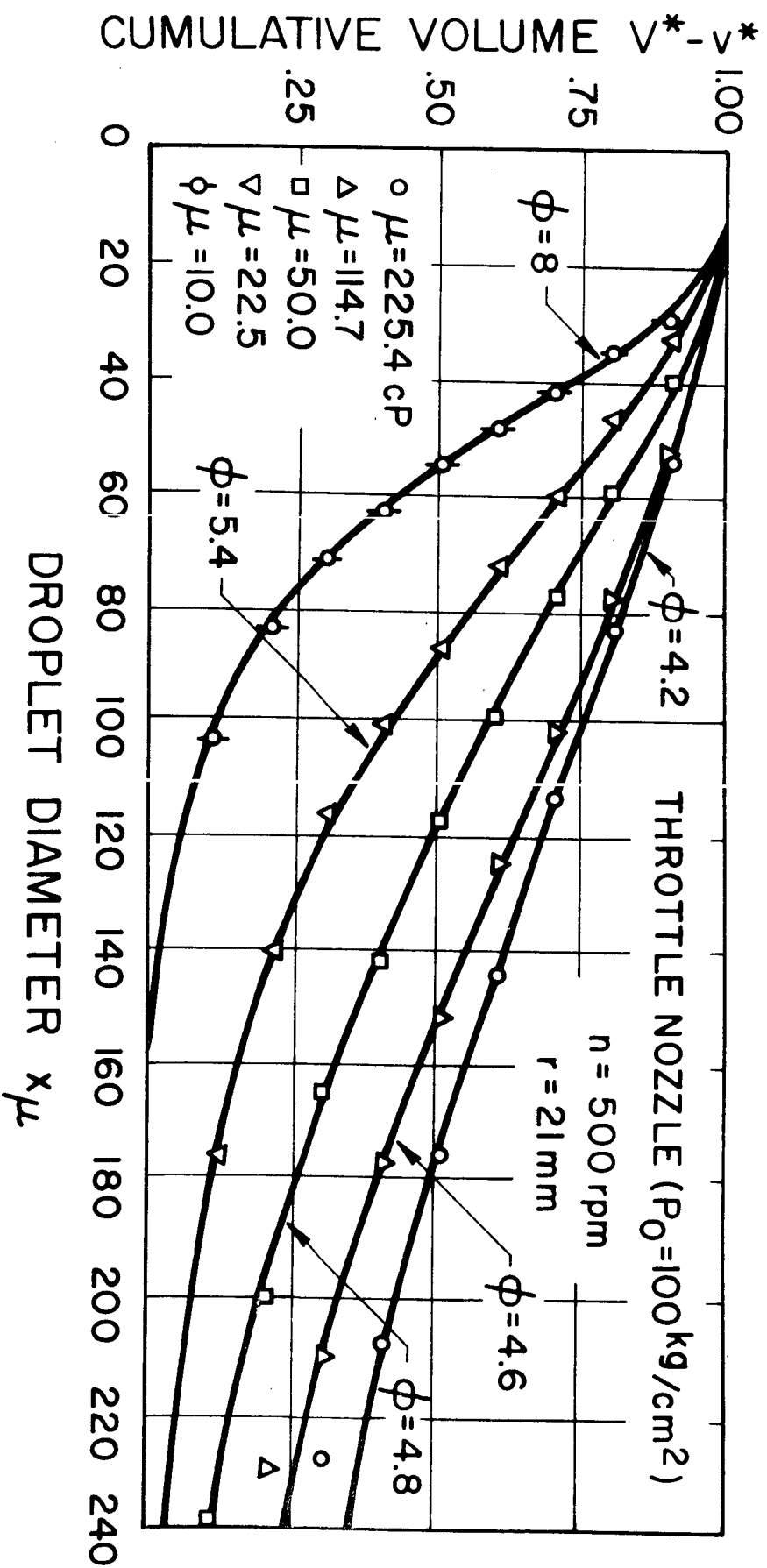◇ μ=10.0

φ=8
φ=5.4
φ=4.2
φ=4.6
φ=4.8

DROPLET DIAMETER xμ

Fig.22

DISTRIBUTION LIST FOR CONTRACTOR REPORT

Applied Physics Laboratory
The Johns Hopkins University
Attn: W.G. Berl
8621 Georgia Avenue
Silver Spring, Maryland 20910

Chemical Propulsion Information Agency
Attn: T.W. Christian
8621 Georgia Avenue
Silver Spring, Maryland 20910

Rocketdyne
A Div. of North American Aviation
Attn: E.C. Clinger
6633 Canoga Avenue
Canoga Park, California 91304

NASA
Lewis Research Center
Attn: E.W. Conrad
21000 Brookpark Road
Cleveland, Ohio 44135

U.S. Naval Ordnance Test Station
Attn: D.Couch
China Lake, California 93555

Multi-Tech., Inc.
Attn: F.B. Cramer
601 Glenoaks Blvd.
San Fernando, California 91340

Aerospace Corporation
Attn: O.W. Dykema
P.O. Box 95085
Los Angeles, California 90045

Ohio State University
Dept. of Aeronautical & Astronautical
   Engineering
Attn: R. Edse
Columbus, Ohio 43210

TRW Systems
Attn: G.W. Elverum
1 Space Park
Redondo Beach, California 90278

The Pennsylvania State University
Mechanical Engineering Department
Attn: G.M. Faeth
207 Mechanical Engineering Bldg.
University Park, Pennsylvania, 16802

University of Southern California
Dept. of Mechanical Engineering
Attn: M. Gerstein
University Park
Los Angeles, California 90007

Princeton University
Forrestal Campus
Guggenheim Laboratories
Attn: I. Glassman
Princeton, New Jersey 08540

Defense Research Corporation
Attn: B. Gray
P.O. Box 3587
Santa Barbara, California 93105

Research & Technology Division
Air Force Systems Command
Attn: L. Green, Jr. (RTGS)
Bolling AFB, Washington, D.C.
                            20332

Princeton University
Forrestal Campus
Guggenheim Laboratories
Attn: D. Harrje
Princeton, New Jersey 08540

Aerojet-General Corporation
Attn: R.J. Hefner
P.O. Box 15847
Sacramento, California 95809

Dynamic Science Corporation
Attn: R.J. Hoffman
1900 Walker Avenue
Monrovia, California 91016

Office of Naval Research
Navy Department
Attn: R.D. Jackel, 429
Washington, D.C. 20360

Rocketdyne
A Div. of North American Aviation
Attn: R.B. Lawhead
6633 Canoga Avenue
Canoga Park, California 91304

Contractor Report Distribution List

NASA
Headquarters
Attn: R.S. Levine, Code RPL
6th & Independence Avenue, S.W.
Washington, D.C. 20546

Pratt & Whitney Aircraft
Florida Research & Development Ctr.
Attn: G.D. Lewis
P.O. Box 2691
West Palm Beach, Florida 33402

Thiokol Chemical Corporation
Reaction Motors Division
Attn: D. Mann
Denville, New Jersey   07834

Dartmouth University
Attn: P.D. McCormack
Hanover, New Hampshire   03755

University of Michigan
Aerospace Engineering
Attn: J.A. Nicholls
Ann Arbor, Michigan 48104

University of California
Department of Chemical Engineering
Attn: A.K. Oppenhiem
6161 Etcheverry Hall
Berkeley, California   94720

Purdue University
School of Mechanical Engineering
Attn: J.R. Osborn
Lafayette, Indiana   47907

United Technology Center
Attn: R.H. Osborn
P.O. Box 358
Sunnyvale, California   94088

U.S. Naval Ordnance Test Station
Attn: E.W. Price, Code 508
China Lake, California 93555

NASA Lewis Research Center
Attn: R.J. Priem, MS-86-5
21000 Brookpark Road
Cleveland, Ohio 44135

Sacramento State College
Engineering Division
Attn: F.H. Reardon
60000 J. Street
Sacramento, California 95819

NASA
George C. Marshall Space Flight Ctr
R-P&VE-PA, Attn: R.J. Richmond
Huntsville, Alabama 35812

Bell Aerosystems Company
Attn: T.G. Rossmann
P.O. Box 1
Buffalo, New York 14205

Jet Propulsion Laboratory
California Institute of Technology
Attn: J.H. Rupe
4800 Oak Grove Drive
Pasadena, California 91103

University of California
Mechanical Engineering, Thermal Sys
Attn: R. Sawyer
Berkeley, California 94720

ARL(ARC)
Attn: K. Scheller
Wright-Patterson AFB
Dayton, Ohio 45433

NASA Manned Spacecraft Center
Attn: J.G. Thibadaux
Houston, Texas 77058

Geophysics Corporation of America
Technology Division
Attn: A.C. Tobey
Burlington Road
Bedford, Massachusetts   01730

Massachusetts Institute of
     Technology
Dept. of Mechanical Engineering
Attn: T.Y. Toong
Cambridge, Massachusetts 02139

Illinois Institute of Technology
RM 200 M.H.
Attn: T.P. Torda
3300 S. Federal Street
Chicago, Illinois 60616

Contractor Report Distribution List

The Warner & Swasey Company
Control Instrument Division
Attn: R.H. Tourin
32-16 Downing Street
Flushing, New York 11354

United Aircraft Corporation
Research Labs.
Attn: D.H. Utvick
400 Main Street
East Hartford, Connecticut 06108

AFRPL (RPRR)
R.R. Weiss
Edwards, California 93523

U.S. Army Missile Command
AMSMI-RKL, Attn: W.W. Wharton
Redstone Arsenal, Alabama 35808

Air Force Office of Scientific Research
Attn: B.T. Wolfson 1400 Wilson Blvd.
Arlington, Virginia 22209

Georgia Institute of Technology
Aerospace School
Attn: B.T. Zinn
Atlanta, Georgia 30332

NASA
Lewis Research Center
Attn: P.R. Wieber, MS-86-5
21000 Brookpark Road
Cleveland, Ohio, 44135

Office of Grants and Research
     Contracts
NASA
Washington, D.C. 20546

NASA Lewis Research Center
21000 Brookpark Road
Cleveland, Ohio 44135
Attn: Paul Wieber (3) MS-7-1
      Library   (2) MS-60-3
      Report Control Office (1)